

Harlay J.<sup>1</sup>, Borges A.V.<sup>2</sup>, De Bodt C.<sup>1</sup>, d'Hoop Q.<sup>1</sup>, Piontek J.<sup>3</sup>, Røevros N.<sup>1</sup>, Suykens K.<sup>2</sup>, Van Oostende N.<sup>4</sup>, Engel A.<sup>3</sup>, Groom S.<sup>5</sup>, Sabbe K.<sup>4</sup>, and Chou L.<sup>1</sup>.

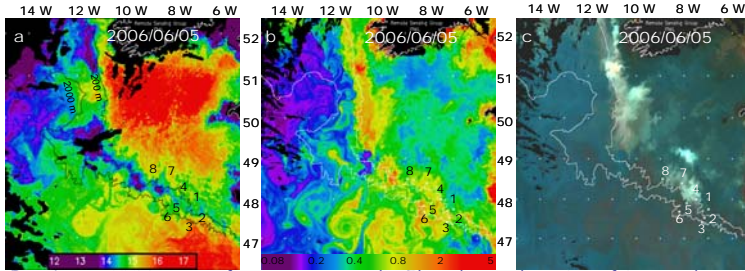


Fig. 1: a- AVHRR sea surface temperature (SST) in the northern Bay of Biscay, showing the location of the stations, the 200 m and 2000 m isobaths, b- SeaWiFS chlorophyll-a (Chl-a) and c- SeaWiFS reflectance satellite images.

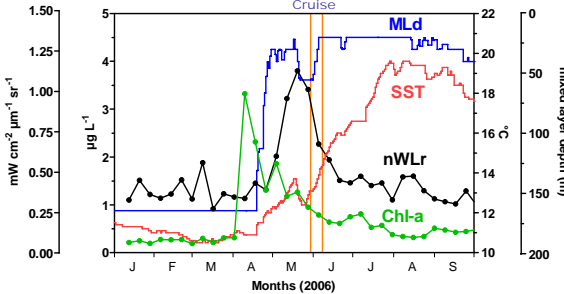


Fig. 2: Time series of remote sensed weekly Chl-a concentrations and normalized water-leaving radiance @555 nm (nWLR), modelled daily mixed layer depth (MLD) and SST in the studied area from January to September 2006. Chl-a and nWLR are Level-3 SeaWiFS data (<http://reason.gsfc.nasa.gov/Giovanni/>) and MLD and SST were simulated with Met Office National Centre for Ocean Forecasting for the North-East Atlantic 1/8° model (<http://www.nerc-essc.ac.uk/godiva/>).

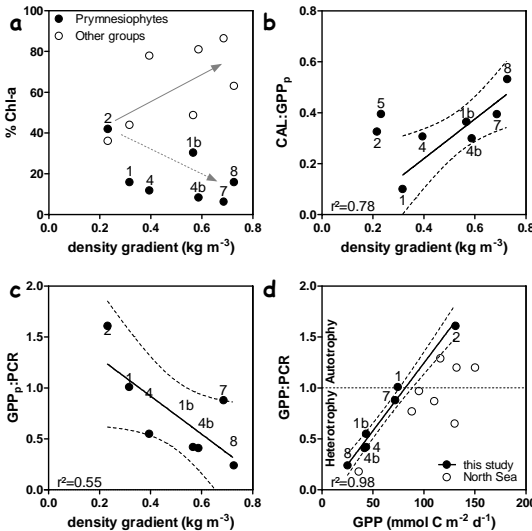


Fig. 3: a- Depth averaged HPLC relative percentage of Pymnesiophytes (filled circles) and other phytoplankton groups (open circles) in the 30 m top layer, b- calcification to gross particulate primary production (CAL:GPP<sub>p</sub>) ratio and c- GPP<sub>p</sub> to pelagic respiration (GPP<sub>p</sub>:PCR) ratio versus the degree stratification computed as the difference of density at 3 m depth and at 100 m depth. The linear regression and the 95% confidence interval (dashed curves) are represented together with the determination coefficient (r<sup>2</sup>). d- GPP<sub>p</sub>:PCR ratio versus GPP in June 2006 in the Bay of Biscay (filled circles) and in June 1999 (open circles) for the North Sea (Robinson *et al.*, 2002).

**INTRODUCTION**

During coccolithophorid blooms, carbon (C) cycling in the photic zone is driven by the production and the degradation of organic matter (primary production and community respiration), and the production and the dissolution of biogenic calcite (CaCO<sub>3</sub>). Organic and inorganic metabolisms lead to a transfer of carbon to depth and both impact the flows of carbon dioxide (CO<sub>2</sub>) into the water column and CO<sub>2</sub> flux across the air-sea interface. Further, due to complex dynamics of coccolithophores, the impact of metabolic C fluxes on CO<sub>2</sub> fluxes is variable in time, depending on the bloom development phase, and mainly dependant on the ratio of calcification to primary production (CAL:GPP ratio). Understanding and quantifying C cycling of coccolithophorid blooms in natural conditions is a prerequisite to correctly validate biogeochemical models that aim at predicting feedbacks related to ocean acidification incorporating knowledge obtained from perturbation laboratory experiments.

We carried out a trans-disciplinary cruise on board the R/V *Belgica* at the continental margin of the Bay of Biscay in June 2006 (Fig. 1), in a coccolithophorid bloom, during which <sup>14</sup>C primary production (GPP<sub>p</sub>), <sup>14</sup>C calcification (CAL) and O<sub>2</sub>-based pelagic respiration rates (PCR) were determined in the water column.

Table 1: Carbon fluxes [mmol C m<sup>-2</sup> d<sup>-1</sup>] based on a mass balance where the <sup>14</sup>C incubations are assumed to correspond to gross primary production (GPP<sub>p</sub>), where pelagic community respiration (PCR) is the sum of autotrophic and heterotrophic respiration based on oxygen incubations converted to C units using a respiratory quotient of 1, and where CAL is the rate of calcification based on <sup>14</sup>C incubations.

Station	Date	pCO <sub>2</sub>	Rate measurements			CO <sub>2</sub> Fluxes			C fluxes			
			GPP <sub>p</sub>	CAL	PCR	GPP <sub>p</sub>	CAL	PCR	Net CO <sub>2</sub> flux based on metabolic rates	Net CO <sub>2</sub> on measured pCO <sub>2</sub>	Export	Aphotic C demand
5	2 June	320	74.2	24.2	-	-74.2	14.5	-	-	-9.1	-	-
2	1 June	306	130.8	51.7	81.3	-130.8	31.0	81.3	-18.5	-11.4	49.5	89.0
1	31-May	265	74.2	7.5	73.7	-74.2	4.5	73.7	4.0	-17.8	0.5	98.2
4 (HR)	2 June	293	43.3	13.3	78.9	-43.3	8.0	78.9	43.6	-13.4	-35.6	66.9
1b	9 June	273	43.3	15.8	103.5	-43.3	9.5	103.5	69.7	-16.1	-60.2	159.0
4b (HR)	8 June	307	41.7	12.5	101.2	-41.7	7.5	101.2	67.0	-10.7	-59.5	168.5
7 (HR)	7 June	309	71.7	28.3	81.4	-71.7	17.0	81.4	26.7	-10.2	-9.7	35.1
8 (HR)	6 June	325	25.0	13.3	104.3	-25.0	8.0	104.3	87.3	-8.5	-79.3	72.3

**RESULTS**

The time series of remotely sensed parameters reveals a rise of SST accompanied by a shoaling of the thermocline to 25 m depth during the period of the cruise (Fig. 2). This situation is favourable for coccolithophore development, as indicated by elevated nWLR, moderate (~1 μg L<sup>-1</sup>) Chl-a concentration (Fig. 2) and nutrient exhaustion (not shown).

In agreement with Margalef's Mandala, the degree of stratification was hypothesized to control biological processes and allowed reconstructing the bloom succession phases of the coccolithophore-dominated bloom (Fig. 3). Bloom aging was characterized by a decrease of Pymnesiophyte biomass relative to other phytoplankton groups (Fig. 3a). With increasing stratification from early coccolithophorid bloom stations (1-2-5) to the later stages (station 8), GPP<sub>p</sub> decreased as CAL increased over the shelf, leading to a significant CAL:GPP<sub>p</sub> ratio for later stages of the bloom (Fig. 3b). The aging of the bloom lead to a lower GPP<sub>p</sub>:PCR ratio (Fig. 3c) and an evolution from net phytoplanktonic community autotrophy to net heterotrophy (Fig. 3d). Consistency of this ratio was checked against Robinson *et al.* (2002) in the North Sea (Fig. 3d).

A C-budget was computed along a gradient from the productive (station 2) to the high reflectance zone (station 8). Surface waters remained as a net sink for atmospheric CO<sub>2</sub> (Table 1), although TA data (not shown) indicated that calcification had a large impact on surface carbonate chemistry. However, net autotrophy was only found for the early phase of the bloom (station 2) where the potential export was of the same magnitude as the aphotic C demand. In other cases, the C export was neutral or negative and insufficient to sustain aphotic demand.

**CONCLUSIONS**

Our classical C-budgeting approach suffers from several caveats. Firstly, steady state is assumed but C production and degradation are decoupled in time and space, as well as biomineralization and dissolution. Secondly, the importance of dissolved production (GPP<sub>d</sub>) is not considered, here. The importance of GPP<sub>d</sub> and its potential fate into transparent exopolymer particles (TEP) is likely a significant C flux (12% of the POC, Harlay *et al.*, 2009) to sustain the heterotrophic C demand in the twilight zone, as suggested by Koeve (2005).

The estimate of GPP<sub>d</sub> from the particulate nitrogen to carbon ratio in surface waters, based on parameterization by Joassin *et al.* (2008) and the computation of C budget based on GPP<sub>tot</sub> (GPP<sub>tot</sub> = GPP<sub>d</sub> + GPP<sub>p</sub>) contributes to better balanced C fluxes to the twilight zone by providing a net export of the same magnitude than aphotic demand (Harlay *et al. in prep.*)